*American Mineralogist, Volume 77, pages 1021–1030, 1992*

# Water, $CO_2$, Cl, and F in melt inclusions in phenocrysts from three Holocene explosive eruptions, Crater Lake, Oregon

CHARLES R. BACON
U.S. Geological Survey, 345 Middlefield Road, Menlo Park, California 94025, U.S.A.
SALLY NEWMAN, EDWARD STOLPER
Division of Geological and Planetary Sciences, California Institute of Technology, Pasadena, California 91125, U.S.A.

## ABSTRACT

Rare melt inclusions ~100 μm in diameter trapped near the boundaries of corroded patchy zones in plagioclase phenocrysts from Plinian pumice of three Holocene eruptions were analyzed by IR spectroscopy for molecular $H_2O$, OH groups, and $CO_2$ and by electron microprobe for Cl and F. The three rhyodacitic eruptions, each of which began with a Plinian phase, occurred over ~200 yr. The Llao Rock and Cleetwood eruptions ended with degassed lava flows and the subsequent climactic eruption with voluminous ignimbrite. Groundmass glass and melt inclusion compositions (anhydrous) are similar. Inclusions with total $H_2O$ concentrations of 1.2–3.4 wt% are adjacent to fractures or are hourglass inclusions, suggesting partial degassing caused by depressurization. Melt inclusions in phenocrysts in climactic ignimbrite may have vesiculated for the same reason. Intact inclusions in Plinian pumices have total $H_2O$ concentrations believed to represent magmatic $H_2O$ contents (wt%): Llao Rock, 5.3, 5.3; Cleetwood, 3.8, 4.7; climactic 3.9 ± 0.2 ($1\sigma$, $n = 6$). Ratios of OH/molecular $H_2O$ indicate closure temperatures of 200–500 °C that reflect syn- or posteruptive cooling. $CO_2$ concentrations are ≤25 ppm. $H_2O$ and $CO_2$ concentrations indicate saturation pressures of 1.0–1.8 kbar or depths ≥5 km. Six inclusions from climactic pumice average 400 ± 40 ($1\sigma$) ppm F, 1880 ± 70 ppm Cl. F and Cl concentrations of the other samples are similar and not well correlated with each other or with total $H_2O$.

Location of melt inclusions near boundaries of patchy zones, which are mantled by oscillatory-zoned overgrowths, suggests that their $H_2O$ concentrations represent magmatic values significantly before eruption. Although mean $H_2O$ concentrations of analyzed melt inclusions decrease for the three successive eruptions, it is not certain that this indicates a corresponding change in magmatic $H_2O$ content during the interval between eruptions.

## INTRODUCTION

Melt inclusions in phenocrysts of volcanic rocks are believed in many instances to preserve magmatic concentrations of dissolved volatile components. In such cases, preeruption processes, such as fractional crystallization and degassing, can be followed by studying the chemical compositions of melt inclusions. In addition, the minimum pressure of entrapment (therefore of crystallization) can be determined from the dissolved volatile compositions if the system was vapor saturated at the time of entrapment. However, it is essential to know the time of entrapment and the subsequent history of the liquid now preserved as glass in order to interpret data from melt inclusions correctly.

The primary goal of most studies of dissolved volatiles in melt inclusions has been to quantify preeruptive magmatic volatile contents. Dissolved volatile concentrations in melt inclusions in bulk samples of quartz phenocrysts from the Bandelier Tuff were determined by Sommer (1977); see also Sommer and Schramm (1983). Data for individual melt inclusions were first reported by Harris and Anderson (1983, 1984). Recently, use of infrared spectroscopy and the ion microprobe has facilitated measurements on individual inclusions (Anderson et al., 1989; Dunbar et al., 1989; Hervig et al., 1989; Newman and Chesner, 1989; Vogel et al., 1989; Webster and Duffield, 1991; Lowenstern and Mahood, 1991). A common conclusion of modern studies is that preeruptive magmatic volatile concentrations have less influence on eruptive style (i.e., explosive eruption vs. quiet effusion) than decompression history, which controls subsurface degassing behavior. Data for melt inclusions have also allowed estimates of minimum depths to reservoirs, assuming gas saturation, and in some cases have led to the conclusion that magmas were vapor saturated during phenocryst growth (Anderson et al., 1989). Our study attempts to document preeruptive magmatic volatile contents based on analysis of melt inclusions in plagioclase phenocrysts.

In this study we report infrared spectroscopic and electron probe microanalyses of melt inclusions in plagio-

0003–004X/92/0910–1021$02.00

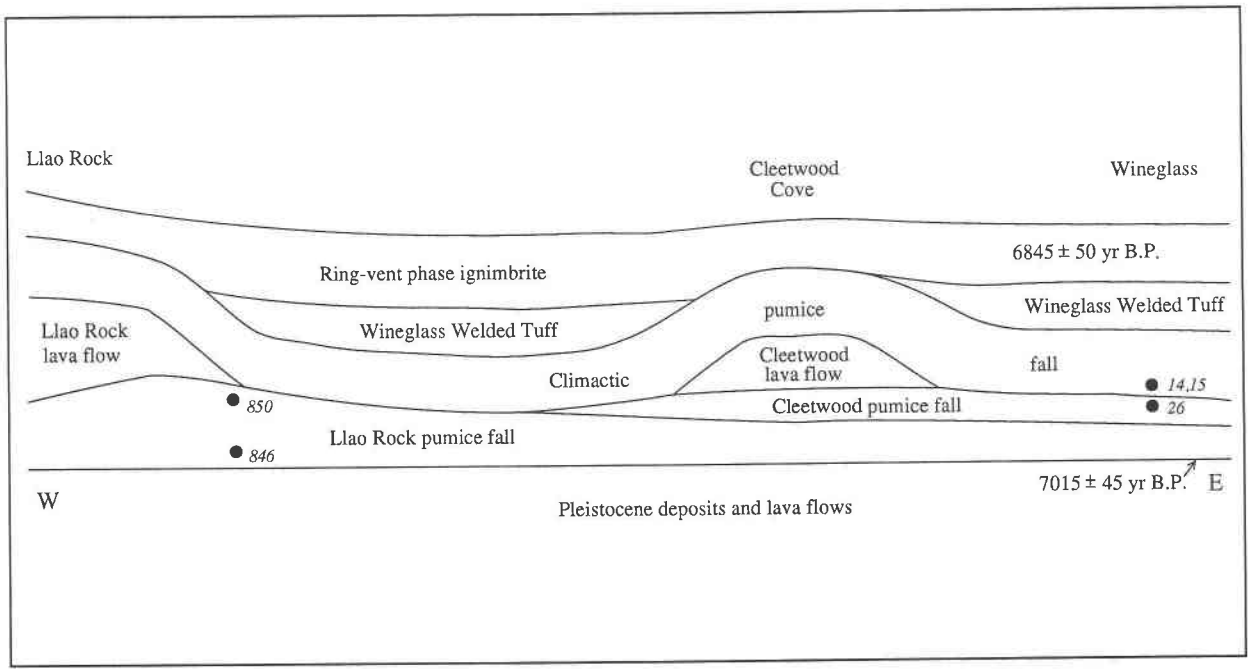


Fig. 1. Schematic stratigraphic relations between Holocene preclimactic and climactic eruption pryoclastic deposits and lava flows along the north rim of Crater Lake caldera. Numbers indicate localities for pumice samples from which melt inclusions were analyzed. Not to scale.

clase from pumices of three Holocene eruptions at Mount Mazama (Crater Lake), Oregon. Much volcanological and petrological information exists for these eruptions (Bacon and Druitt, 1988; Druitt and Bacon, 1986, 1989; Young, 1990), and their timing is relatively well known (Bacon, 1983). All began with an explosive Plinian phase. The first two ended with degassed lava flows, the third with collapse of Crater Lake caldera during the climactic eruption, which ejected ~50 km$^3$ of magma. Our study focuses on Plinian pumices with melt inclusions whose dissolved volatile concentrations are believed to represent magmatic values at times significantly before each Plinian eruption began. The melt inclusion data provide information about points in the magmas' history and constrain minimum depths for magma reservoirs. We also discuss volatile concentrations in glass in vitrophyres from one of the late-stage lava flows and some implications of the vesiculation of melt inclusions in phenocrysts from the climactic eruption.

## Geology

Mount Mazama is one of the major Quaternary volcanic centers of the High Cascades. It consists of a complex of basaltic andesitic to dacitic shields and stratovolcanoes constructed between ~420 000 and ~40000 years ago (Bacon, 1983; Bacon and Lanphere, 1990). Rhyodacitic volcanism related to growth of the climactic magma chamber began ~30000 years ago, producing several preclimactic lava flows and domes, at least some of which were preceded by small Plinian eruptions. The samples we have studied are from the Llao Rock and Cleetwood preclimactic eruptions and the climactic eruption itself.

Products of the Llao Rock event consist of two dikes in the caldera wall, a mildly zoned Plinian deposit, and a thick lava flow (Fig. 1). Charcoal fragments from beneath the Plinian deposit gave a $^{14}$C age of 7015 ± 45 yr B.P. (Bacon, 1983). The Cleetwood eruption is represented by a Plinian deposit and an overlying lava flow. The Cleetwood lava flow was still hot, and plastic in its interior, at the time of the climactic eruption. The climactic eruption began with a Plinian column that collapsed to form the Wineglass Welded Tuff (Williams, 1942) ignimbrite that is found on the north and east flanks of Mazama; the Plinian deposit and the Wineglass originated from a single vent and are nearly entirely rhyodacite. Eruption of the Wineglass ended when the caldera began to collapse. Caldera formation was accompanied by emplacement of zoned ignimbrite, dominantly rhyodacite that was followed by andesite and mafic cumulate material, from highly mobile pyroclastic flows that were fed by multiple vents around the perimeter of the subsiding block (Bacon, 1983; Druitt and Bacon, 1986). Bacon (1983) reported a weighted mean $^{14}$C age of 6845 ± 50 yr B.P. for charcoal associated with primary deposits of the climactic eruption.

## Petrology

Compositions of rocks, glasses, and phenocrysts are known for all products of the climactic magma chamber (Bacon and Druitt, 1988; Druitt and Bacon, 1989). The

Llao Rock Plinian deposit is zoned from relatively differentiated rhyodacite at its base to rhyodacite similar to that of the climactic eruption at its top (except for slightly higher Ba and lower Mg and Sr concentrations); Fe-Ti oxide microphenocryst equilibration temperatures are ~860 °C at the base and ~890 °C at the top of the deposit. The overlying lava flow apparently consists of a mixture of these two rhyodacite compositions. Cleetwood pumice and lava are compositionally (anhydrous basis) and mineralogically identical to rhyodacite pumice of the climactic eruption, which is remarkably homogeneous; all glassy samples from these units have Fe-Ti oxide temperatures of ~880 °C, regardless of mode of eruption or vesicularity. We were successful in analyzing intact melt inclusions in plagioclase from late Llao Rock, Cleetwood, and early climactic pumice, all of which have Fe-Ti oxide temperatures of ~880–890 °C.

The rhyodacites studied contain approximately 10 vol% phenocrysts of plagioclase, orthopyroxene, clinopyroxene, hornblende, magnetite, and ilmenite (Druitt and Bacon, 1989). Consistency of phenocryst rim compositions indicates preeruptive equilibrium with melt now represented by groundmass glass. Here we focus on plagioclase because it is the host phase for analyzed melt inclusions. Anorthite and Sr contents of plagioclase can be used to fingerprint individual crystals in terms of their sources in the zoned chamber (Druitt and Bacon, 1989), which contained crystallization products of parent magmas with different Sr concentrations (Bacon and Druitt, 1988). Reverse zoning of Sr concentrations accompanying normal Ab-An zoning of plagioclase is common, reflecting hybridization of magmas. Patchy zoning with little compositional range is present in many phenocrysts, either in cores or in thick zones, which are overgrown by thick, oscillatory zoned rims (Figs. 2a, 2b). The patchy zoning may have resulted from cellular growth of plagioclase (Anderson, 1984) or from resorption. Margins of patchy zones are irregular and rounded suggesting resorption, as is also indicated by truncated oscillatory zones (Fig. 2c) attending magma mixing or temperature increase.

Melt inclusions in plagioclase phenocrysts are most common near the irregular margins of patchy-zoned cores (Figs. 2a, 2b). Inclusions are composed of brown glass, have negative crystal shapes, and are up to ~130 $\mu$m in maximum dimension. Intact inclusions yielded what we consider to be magmatic volatile concentrations. In these, a single or small number of 10–20-$\mu$m bubbles that are commonly present are attributed to shrinkage (ca. 1–2 vol% of an inclusion). No daughter crystals were observed, and there is no evidence for postentrapment crystallization (e.g, no inverse correlation between Ca or Al and Cl or Mg).

Many inclusions, some of which were analyzed, display petrographic evidence for leakage and volatile loss during or after entrapment. For example, very thin ($\leq$2 $\mu$m) capillary tubes connect some inclusions with groundmass glass (Fig. 2d), as in "hourglass" inclusions described by Anderson (1991) in quartz of the Bishop Tuff. In addition, many inclusions have vesiculated and show evidence of having leaked melt, either through capillaries or fractures (cf. St. Seymour and Vlassopoulos, 1989, their Fig. 6; Anderson et al., 1989). Inclusions in all phenocrysts examined from the Wineglass Welded Tuff and the ring-vent phase ignimbrite are of this type. Some inclusions are partially devitrified, and this may have affected the volatile concentrations in their glass.

## Analytical methods

Fresh pumice clasts were selected from deposits of known stratigraphic position. Plagioclase phenocrysts containing melt inclusions large enough for analysis were picked from crystal concentrates made by gently crushing fragments of single pumice clasts and washing away the glass with $H_2O$. Crystals were mounted on glass slides, ground, and polished to expose melt inclusions. Major element compositions of plagioclase and melt inclusions were determined on an automated, five-crystal spectrometer JEOL 733 electron microprobe; in addition, Sr was measured in plagioclase (a correction was made for interference of Si$K\beta$ on Sr$L\alpha$; precision of concentration measurements is $\pm$10% or better) and F and Cl in glass. Microprobe operating conditions were 15 kV accelerating voltage, 12–30-nA beam current, and 20-$\mu$m diameter electron beam. Corrections were calculated using the Citzaf program (Armstrong, 1988) employing the absorption correction of Armstrong (1982), the atomic number correction of Love et al. (1978), and the fluorescence correction of Reed (1965) as modified by Armstrong (1988). Doubly polished wafers were then made from the plagioclase phenocrysts so that individual melt inclusions were exposed on both sides of the crystal. Infrared spectroscopic measurements were made on these inclusions using a Nicolet 60SX Fourier transform (FTIR) spectrophotometer following procedures modified after Newman et al. (1986). The modifications consisted of the use of the microbeam chamber as opposed to the main sample chamber of the 60SX spectrophotometer. Using this chamber increases the signal-to-noise ratio up to 36 times relative to the same conditions in the main chamber because of a 6X condensing lens. The melt inclusions were mounted over 35–50-$\mu$m apertures during the FTIR measurements. Molecular $H_2O$ concentration was determined from the band at ~5200 $cm^{-1}$ and OH at ~4500 $cm^{-1}$; the sum of molecular $H_2O$ + OH calculated as $H_2O$ was checked against total $H_2O$ determined from the band at ~3550 $cm^{-1}$ (Newman et al., 1986). Five vitrophyre samples from the Cleetwood lava flow were also analyzed for total $H_2O$ using the ~3550-$cm^{-1}$ band. The molar absorptivity used for the 3550-$cm^{-1}$ band, the fundamental OH-stretching vibration, was 88 $\pm$ 2 (Dobson et al., 1989). Dissolved molecular $CO_2$ concentration in melt inclusions was obtained from the ~2350-$cm^{-1}$ band. The molar absorptivity used was 1078 (Blank et al., 1989). We assumed that the density of the glasses was 2.3 $g \cdot cm^{-3}$. Two to five analyses were made of each inclusion.

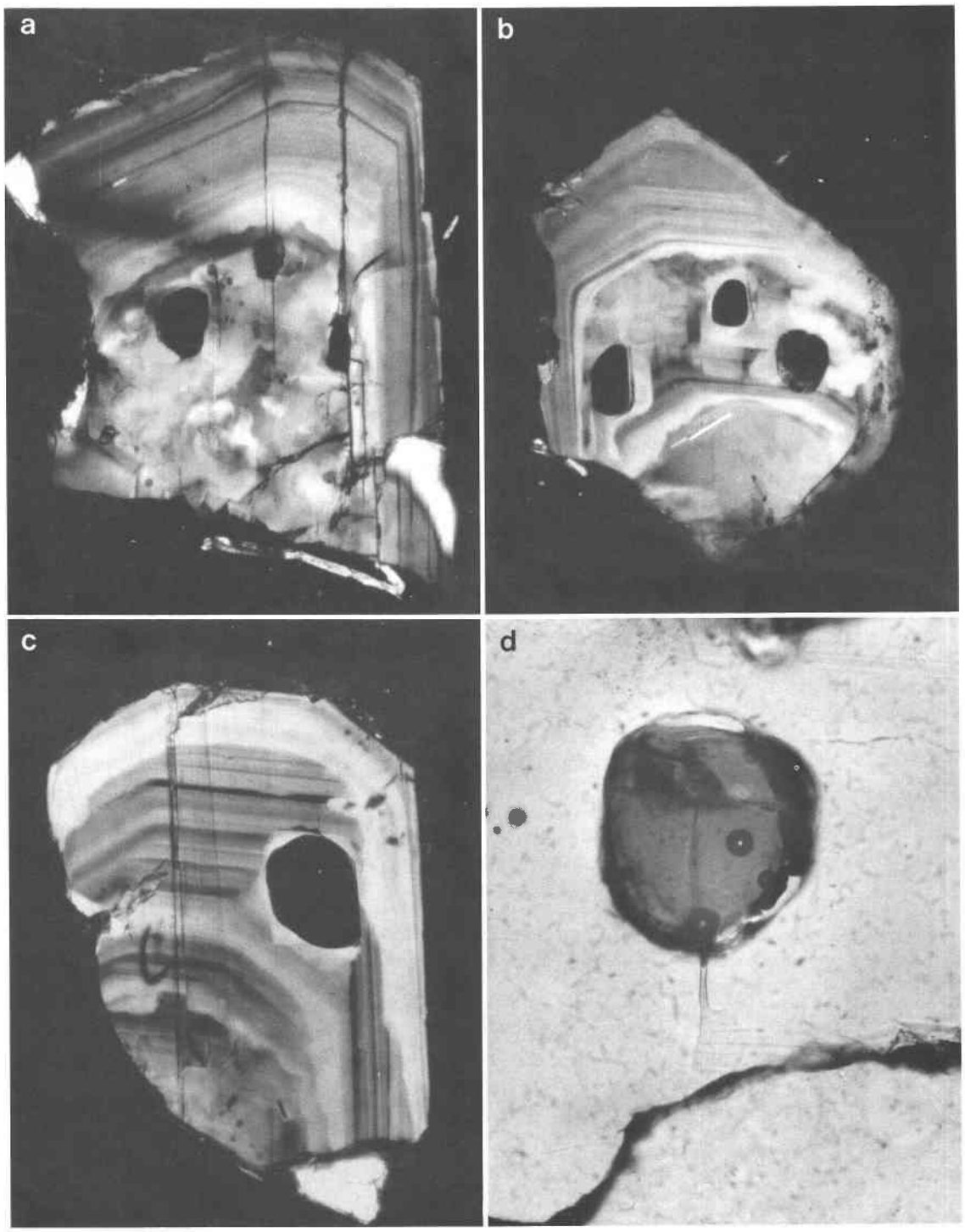


Fig. 2. Photomicrographs of plagioclase phenocryst fragments and melt inclusions from sample 14 from the Plinian deposit of the climactic eruption. (**a**) Patchy-zoned core with melt inclusions near outer edge (crystal 7), overgrown by oscillatory zoned rim. Large melt inclusion is 100 × 130 μm. (**b**) Patchy zone containing melt inclusions between core and oscillatory zoned rim (crystal 5). Elongate melt inclusion is 70 × 130 μm. (**c**) Complex oscillatory zoned crystal showing three unconformities representing resorption followed by renewed growth; melt inclusion is 90 × 120 μm (crystal 6). (**d**) Hourglass melt inclusion (crystal 1). Inclusion is 100 μm across, capillary ~2 μm.

**TABLE 1.** Plagioclase phenocryst compositions

| Unit | Sample | Xtl | An (mol%) | Ab (mol%) | Or (mol%) | Sr (ppm) | Comments |
|---|---|---|---|---|---|---|---|
| Climactic | 14 | 1 | 37.8 | 60.5 | 1.7 | 1080 | by mi |
| | | | 39.2 | 59.3 | 1.4 | 1250 | by mi |
| | | | 37.2 | 61.2 | 1.7 | 1360 | rim |
| Climactic | 14 | 2 | 38.5 | 59.9 | 1.6 | 1100 | by mi |
| | | | 39.5 | 59.1 | 1.4 | 1160 | inner rim |
| Climactic | 14 | 3 | 47.9 | 51.1 | 1.0 | 890 | core |
| | | | 47.9 | 51.0 | 1.1 | 1170 | by mi |
| | | | 45.1 | 53.7 | 1.2 | 1150 | by mi |
| | | | 40.6 | 57.9 | 1.5 | 1140 | inner rim |
| | | | 36.9 | 61.5 | 1.6 | 940 | mid rim |
| | | | 37.4 | 60.9 | 1.6 | 1150 | rim |
| Climactic | 14 | 5 | 38.7 | 59.9 | 1.5 | 1220 | core |
| | | | 40.3 | 58.2 | 1.5 | 1100 | by mi |
| | | | 42.0 | 56.7 | 1.4 | 970 | by mi |
| | | | 38.3 | 60.2 | 1.5 | 1500 | rim |
| Climactic | 14 | 6 | 36.2 | 62.1 | 1.6 | 1010 | core |
| | | | 37.3 | 61.1 | 1.7 | 1160 | by mi |
| | | | 39.2 | 59.2 | 1.6 | 1600 | rim |
| Climactic | 14 | 7 | 42.9 | 55.8 | 1.2 | 1080 | core |
| | | | 40.8 | 57.8 | 1.4 | 960 | by mi |
| | | | 33.9 | 64.2 | 1.9 | 980 | rim |
| Climactic | 15 | 8 | 38.9 | 59.6 | 1.5 | 1050 | by mi |
| | | | 38.6 | 59.9 | 1.5 | 1090 | inner rim |
| | | | 34.4 | 61.7 | 3.8 | 1300 | rim |
| Cleetwood | 26 | 3 | 38.8 | 59.8 | 1.4 | 1110 | core |
| | | | 35.6 | 62.7 | 1.7 | 1070 | inner rim |
| Cleetwood | 26 | 4 | 40.7 | 57.9 | 1.3 | 1040 | core |
| | | | 41.7 | 57.1 | 1.2 | 1280 | rim |
| Llao Rock | 850 | 1 | 39.1 | 59.5 | 1.4 | 990 | core |
| | | | 46.8 | 52.1 | 1.1 | 1190 | rim |
| Llao Rock | 846 | 3 | 38.7 | 60.0 | 1.4 | 1000 | by mi |
| | | | 38.6 | 60.0 | 1.4 | 1100 | core |
| | | | 45.3 | 53.6 | 1.1 | 1470 | rim |

*Note:* Sr concentrations corrected for interference of Si$K\beta$ on Sr$L\alpha$. The abbreviation mi = melt inclusion.

The average standard deviation of the replicate analyses for $H_2O$ was 5% and for $CO_2$ was 35%.

## RESULTS

### Inclusion and host compositions

A necessary, but not sufficient, condition for volatile concentrations in melt inclusions to reflect magmatic conditions in the host magma just prior to eruption is that host crystals must be representative of the phenocryst population and glass compositions must be similar to that of the groundmass glass. Plagioclase compositions adjacent to analyzed melt inclusions are $An_{37-48}$, most being $\sim An_{39}$ (Table 1). Sr concentrations at the same points are 960–1250 ppm but are not directly correlated with An. Rim compositions range from $An_{39}$, 1600 ppm Sr to $An_{34}$, 980 ppm Sr. Comparison of these data with those of Druitt and Bacon (1989) shows that the host crystals for the studied melt inclusions are indeed compositionally representative of phenocrysts in their respective eruptive units.

Major element compositions of melt inclusions determined by electron microprobe are similar to X-ray fluorescence analyses of glass separates from pumices when both are recalculated to total 100 wt% on an anhydrous basis. Mean compositions of melt inclusions (23 spot analyses) in climactic pumice are compared with the mean of five analyses of groundmass glass separates from climactic rhyodacite in Table 2. In general, differences between specific melt inclusion analyses and typical groundmass compositions are small and similar to the reproducibility of the microprobe data. Although we cannot prove that a particular melt inclusion is identical in composition to nearby groundmass glass, the analyzed melt inclusions are representative of liquids in the remarkably homogeneous (Bacon and Druitt, 1988) rhyodacitic part of the magma chamber.

### $H_2O$ concentrations in melt inclusions

Results of FTIR measurements of molecular $H_2O$, OH, and total $H_2O$ concentrations are presented in Table 3. The sum of molecular $H_2O$ and OH calculated as $H_2O$ is believed to be a more accurate value than total $H_2O$ determined from the $\sim$3550-$cm^{-1}$ band at the observed concentrations in melt inclusions; we refer to this sum as total $H_2O$ concentration in what follows, except for the Cleetwood lava flow samples, which contain very little $H_2O$.

A total of three melt inclusions were analyzed in two samples from the Llao Rock pumice fall beneath the east edge of the Llao Rock lava flow, one from the base (846) and one from the top (850). The inclusion in the basal sample gave a low total $H_2O$ concentration (2.1 wt%),

**TABLE 2.** Mean glass compositions, climactic rhyodacite

| | Climactic | | | | Cleetwood | | |
|---|---|---|---|---|---|---|---|
| | Melt incls | 1σ | Pumice glass | 1σ | Melt incls | 1σ | Vitrophyre glass |
| | | | Wt% | | | | |
| $SiO_2$ | 73.0 | 0.4 | 73.2 | 0.8 | 73.6 | 0.4 | 73.8 |
| $Al_2O_3$ | 14.7 | 0.26 | 14.4 | 0.46 | 14.3 | 0.18 | 14.2 |
| FeO* | 1.93 | 0.08 | 1.66 | 0.17 | 1.87 | 0.08 | 1.65 |
| MgO | 0.41 | 0.05 | 0.49 | 0.09 | 0.41 | 0.05 | 0.34 |
| CaO | 1.50 | 0.12 | 1.63 | 0.15 | 1.41 | 0.11 | 1.41 |
| $Na_2O$ | 5.11 | 0.17 | 5.13 | 0.21 | 5.30** | — | 5.26 |
| $K_2O$ | 2.84 | 0.07 | 2.85 | 0.11 | 2.55 | 0.20 | 2.82 |
| $TiO_2$ | 0.36 | 0.06 | 0.42 | 0.02 | 0.39 | 0.03 | 0.40 |
| $P_2O_5$ | 0.06 | 0.02 | 0.09 | 0.01 | 0.04 | 0.03 | 0.08 |
| MnO | 0.05 | 0.01 | 0.05 | 0.01 | 0.05 | 0.01 | 0.06 |
| | | | ppm | | | | |
| Sr | 320 | 150 | 307 | 7 | — | — | 298 |

*Note:* Analyses recalculated to total 100% volatile free. Climactic melt inclusions, average of 23 electron probe analyses from samples 14 and 15 (Caltech JEOL 733); climactic pumice glass, average of five X-ray fluorescence analyses of glass separates from pumice (Bruggman et al., 1987); Cleetwood melt inclusions, average of six electron probe analyses from sample 26 (Caltech JEOL 733); Cleetwood vitrophyre glass, electron probe analysis of groundmass glass in lava sample 160 (USGS ARL SEMQ), Sr by X-ray fluorescence on glass separate (Bruggman et al., 1987).

* Total Fe as FeO.

** $Na_2O$ fixed at 5.30% for recalculation.

apparently owing to visible connection with the outside of the plagioclase. Inclusions from two phenocrysts in the late-erupted sample each gave 5.3 wt% total $H_2O$. The latter values are thought to represent magmatic conditions.

Analyses of melt inclusions in two phenocrysts from a pumice clast (26) from near the top of the Cleetwood pumice fall in the caldera wall at Wineglass yielded total $H_2O$ concentrations of 3.8 and 4.7 wt%. This difference appears to be well outside the precision of measurement.

Two pumice clasts from <1 m above the base of the climactic pumice fall were studied (14, 15; Wineglass locality). Two melt inclusions in sample 15 and one in sample 14 have low total $H_2O$ concentrations (2.4, 3.1, 1.2 wt%, respectively). The two higher values are for inclusions that appear to have leaked into glass-filled cracks in plagioclase that connect the inclusions to the outside of the crystals. The lowest value is for an inclusion that is in communication with groundmass glass by a capillary (Fig. 2d). Another six inclusions from sample 14 range from 3.6 to 4.3 wt% total $H_2O$. We take the mean value of 3.9 ± 0.2 (1σ) wt% for these six to be representative of magmatic $H_2O$ content, since the standard deviation about this value is approximately equivalent to our analytical precision. Note that two nearby inclusions in one phenocryst, where the thickness of the analyzed glass is

**TABLE 3.** Volatile concentrations in melt inclusions in plagioclase phenocrysts from Mount Mazama and in vitrophyre glass from the Cleetwood lava flow

| Unit | Sample | Xtl* | Incl** | $H_2O$ mol wt% (5200 $cm^{-1}$) | $H_2O$ OH wt% (4500 $cm^{-1}$) | $H_2O$† tot wt% | $H_2O$ tot wt% (3550 $cm^{-1}$) | $CO_2$ ppm | F ppm | Cl ppm | Comments |
|---|---|---|---|---|---|---|---|---|---|---|---|
| Climactic | 14 | 1 | 1 | 0.62 | 0.62 | 1.2 | | | 400 | 2100 | |
| Climactic | 14 | 2 | 1 | 2.7 | 1.1 | 3.8 | | 11 | 350 | 1850 | hourglass |
| Climactic | 14 | 3 | 1 | 3.3 | 0.99 | 4.3 | | | 350 | 2000 | |
| Climactic | 14 | 5 | 1 | 2.9 | 0.95 | 3.8 | | | 400 | 1900 | |
| | 14 | 5 | 2 | 3.1 | 0.93 | 4.0 | | | 450 | 1800 | |
| Climactic | 14 | 6 | 1 | 2.7 | 1.0 | 3.6 | | | 400 | 1800 | |
| Climactic | 14 | 7 | 1 | 2.8 | 0.99 | 3.8 | | | 450 | 1850 | hourglass |
| Climactic | 15 | 8 | 1 | 1.8 | 0.62 | 2.4 | | | 300 | 1900 | cracked |
| | 15 | 8 | 2 | 2.1 | 1.0 | 3.1 | | | 500 | 2050 | cracked |
| Cleetwood | 26 | 3 | 1 | 2.5 | 1.3 | 3.8 | 4.0 | 17 | 500 | 1600 | |
| Cleetwood | 26 | 4 | 1 | 3.6 | 1.0 | 4.7 | | 10 | 300 | 1750 | cracked? |
| Llao Rock | 850 | 3 | 1 | 4.3 | 0.97 | 5.3 | 6.0 | | 650 | 1800 | |
| Llao Rock | 850 | 4 | 1 | 4.1 | 1.2 | 5.3 | 5.4 | | 250 | 1850 | |
| Llao Rock | 846 | 3 | 1 | 0.95 | 1.1 | 2.1 | 2.0 | 25 | 300 | 2150 | cracked |
| Cleetwood | 160 | — | — | — | — | — | 0.13 | — | — | 1400 | vitrophyre |
| Cleetwood | 770 | — | — | — | — | — | 0.095 | — | 250 | 1100 | vitrophyre |
| Cleetwood | 771 | — | — | — | — | — | 0.077 | — | 500 | 900 | vitrophyre |
| Cleetwood | 779 | — | — | — | — | — | 0.11 | — | 400 | 1150 | vitrophyre |

*Note:* $H_2O$, OH, and $CO_2$ by infrared spectroscopy; F and Cl by electron microprobe (see text).

* Crystal number.

** Inclusion number.

† $H_2O_{mol}$ + OH as $H_2O$.

comparable and thus is not a factor in relative analytical precision, gave 3.8 and 4.0 wt% total $H_2O$.

### $CO_2$ in melt inclusions

It was difficult to obtain molecular $CO_2$ data for the Crater Lake melt inclusions because of the low concentration of this species. We detected $CO_2$ in four inclusions, with values ranging from 10 to 25 ppm. The data are not sufficiently precise or abundant to allow discrimination of any differences that might be present between melt inclusions in pumice from the three eruptive units.

### Cl and F in melt inclusions

There is little variation in Cl among melt inclusions. Ranges for inclusions from preclimactic and climactic pumices are similar: 1750–2150 and 1850–2100 ppm, respectively. Mean values are virtually identical. Cl concentration can be determined with good precision (ca. ±100 ppm, or better, here) with the electron microprobe, suggesting that extreme values, at least, represent true differences in Cl concentration. Cl concentration is not correlated with F, total $H_2O$, or eruptive sequence.

Microprobe analyses for F vary between 270 and 630 ppm. The variation in F appears to be random, and we suspect that most, if not all, can be ascribed to poor analytical precision, largely as a result of determination of background intensities in the presence of overlaps with multiple order Fe and Mg peaks. Like Cl, mean values for F in climactic and preclimactic samples are similar (~400 ppm). Interestingly, Cl and F concentrations in low-$H_2O$ melt inclusions are not significantly lower than those of melt inclusions that appear to have retained magmatic levels of $H_2O$. In contrast, Anderson et al. (1989) reported decreased Cl concentrations in hourglass and cracked inclusions in the Bishop Tuff. Retention of Cl in the Crater Lake inclusions may be a result of shorter duration of the Crater Lake Plinian eruptions and the fact that some of the Bishop Tuff inclusions were from late-erupted ignimbrite.

### Volatile concentrations in Cleetwood vitrophyre glass

Glass in four porphyritic vitrophyre samples from widely separated localities on the surface of the Cleetwood lava flow was analyzed for total $H_2O$, F, and Cl (Table 3). Results are typical of nonhydrated, degassed glassy rhyolitic lava. The range of values is 770–1280 ppm $H_2O$, with a mean of 1000 ± 180 ($1\sigma$) ppm. The average concentrations of Cl and F are 1100 ppm, lower than those of the inclusions, and 320 ppm, similar to those of the inclusions, respectively.

The identical mineral content and anhydrous composition of Cleetwood samples and climactic pumice, their vent locations, and the timing of eruptions suggest that the two eruptions tapped the same rhyodacitic magma. The Cleetwood vitrophyre is part of a lava flow that presumably degassed through loss of a dominantly aqueous vapor phase during ascent and eruption. Cleetwood vitrophyre glass and melt inclusions in Cleetwood and climactic pumices have indistinguishable F concentrations, but the melt inclusions have ~1.5× the Cl and 40× the $H_2O$. The different behavior of F and Cl is qualitatively consistent with experimental studies of F and Cl partitioning between silicate melt and aqueous fluid (Webster and Holloway, 1990). The $H_2O$ concentration in the vitrophyre glass is a result of open-system degassing, as described by Newman et al. (1988).

## Discussion

### Magmatic dissolved volatile concentrations

The general consistency of total $H_2O$ concentrations for intact melt inclusions from a particular eruptive unit suggests these represent preeruptive magmatic $H_2O$ contents. There is some question, however, as to the point in a magma's history when melt inclusions were trapped. Herein lies an advantage of the plagioclase host, where zonation is observable, over the more readily prepared quartz of most other studies of inclusions in silicic magmas: The location of inclusions near the margins of patchy zoned cores of plagioclase phenocrysts (Fig. 2) suggests entrapment was associated with at least one major contamination, mixing, or heating event. Sr concentrations in plagioclase rims (Table 1) are generally higher than in cores, suggesting that resorption of the patchy zones occurred during early Holocene introduction of a new batch of parent magma relatively rich in Sr (Druitt and Bacon, 1989). The uniformity of major element glass compositions among inclusions and groundmasses and the mineral content of the samples imply little change in conditions between entrapment and eruption, regardless of the elapsed time. There is a suggestion of secular decrease in magmatic $H_2O$ content in the order of decreasing age of the samples, spanning what is believed to have been ~200 yr (Bacon, 1983). Given the similar phenocryst content and mineral content of the studied pumices, however, it seems unlikely that melt inclusions record the evolving $H_2O$ concentrations in melt during this period. On the other hand, if intracrystalline diffusion of $H_2O$ in plagioclase is as rapid as $H_2O$ diffusion in quartz may be (so that melt inclusions reequilibrate with external magma in a period measured in years), inclusion $H_2O$ concentrations may indeed reflect magmatic $H_2O$ values effectively at the times of eruption (Qin et al., 1992). In this case, the inclusions in plagioclase phenocrysts in climactic pumice may have adjusted their $H_2O$ concentration by intracrystalline diffusion in the ~200 yr between the Llao Rock and climactic eruptions. We might speculate that the small variation in melt inclusion $H_2O$ concentration in Cleetwood and climactic phenocrysts may be due to different diffusion path lengths for inclusions, reflecting incomplete reequilibration, but we have found no correlation between $H_2O$ concentration and apparent minimum distance from inclusion to crystal margin as measured in photomicrographs of doubly polished wafers (accurate measurement of minimum diffusion path would require determination before polishing). In any case, be-

**TABLE 4.** Calculated saturation pressures and minimum depths

| $H_2O$ (wt%) | $P_{sat}$ (bars) ($CO_2$ = 0 ppm) | Depth (km) | $P_{sat}$ (bars) ($CO_2$ = 50 ppm) | Depth (km) |
|---|---|---|---|---|
| 3.8 | 988 | 4.6 | 1095 | 5.1 |
| 3.9 | 1036 | 4.8 | 1143 | 5.3 |
| 4.7 | 1446 | 6.7 | 1557 | 7.2 |
| 5.3 | 1788 | 8.3 | 1900 | 8.8 |

*Note:* Assumptions for calculations include rhyolite speciation for $H_2O$, rhyolite solubilities for $H_2O$ and $CO_2$, 880 °C, density of overburden = 2.2 g·cm$^{-3}$. See Newman et al. (1988) for details.

cause all of our samples have analytically indistinguishable Fe-Ti oxide equilibration temperatures that must reflect conditions shortly before eruption, we suspect that the different $H_2O$ concentrations in intact melt inclusions resulted from entrapment, or possibly reequilibration, at different times or depths in the magma reservoir.

We accept 3.9–5.3 wt% $H_2O$, <25 ppm $CO_2$, ~400 ppm F, and 1800–2100 ppm Cl as typical of volatile compositions represented by climactic, Cleetwood, and late Llao Rock rhyodacitic magmas. The lower limit of 3.9 wt% $H_2O$ is probably most representative, at least of climactic and Cleetwood magma, because it is based on several measurements from samples typical of the greatest erupted volume of magma and is in agreement with the ~4 wt% estimated by Bacon and Druitt (1988) on the basis of glass composition (Merzbacher and Eggler, 1984). Dacite from Mount St. Helens contains the same phenocryst assemblage as the Mazama rhyodacites, and both have broadly similar glass compositions (the dacite from Mount St. Helens has a greater phenocryst content and its glass is more calcic and less potassic than the Mazama examples). Electron microprobe analysis of melt inclusions in Mount St. Helens phenocrysts and experimental duplication of phase relations indicate 5.0 ± 0.5 wt% $H_2O$ in the liquid (Rutherford et al., 1985; Rutherford and Devine, 1988), which is within the range of measured $H_2O$ concentrations in melt inclusions from Crater Lake.

The preeruptive volatile concentrations in rhyodacitic magma at Crater Lake are similar to the electron (Cl) and ion microprobe results of Dunbar et al. (1989) for $H_2O$, F, and Cl in melt inclusions in phenocrysts of the Taupo and Hatepe Plinian tephras from the Taupo Volcanic Zone, New Zealand. Hervig et al. (1989) presented the same type of data for air-fall tephra from Obsidian Dome near Long Valley, California, in which volatile concentrations are variable but average 4.1 wt% $H_2O$; many F values are notably higher, and Cl lower, than those for Plinian pumices from Crater Lake and the Taupo Volcanic Zone. Anderson et al. (1989) studied melt inclusions in Plinian and ash-flow pumice from the Bishop Tuff, finding typically higher $H_2O$ (5–6 and 4–5 wt%, respectively) and $CO_2$ but lower Cl concentrations than present in the Mazama samples. Melt inclusions in phenocrysts from the Bandelier Tuff (Hervig and Dunbar, 1989) have mean $H_2O \leq 4.7$ wt%, Cl somewhat higher

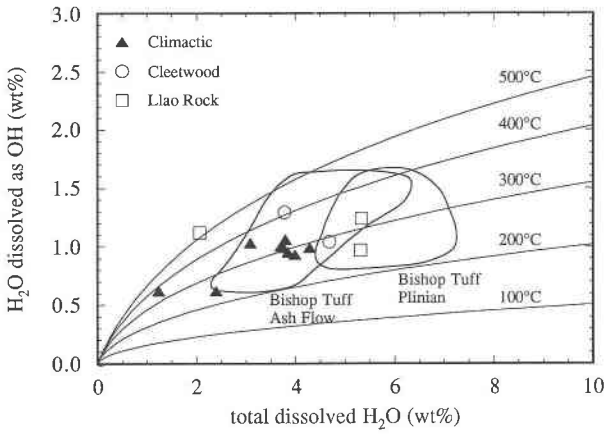


Fig. 3. Molecular $H_2O$ concentrations in melt inclusions plotted against total $H_2O$ concentration and showing $H_2O$ speciation equilibration temperature from Zhang et al. (1991). Fields for the Bishop Tuff from data given by Anderson et al. (1989) and Skirius (1990).

(up to 2900 ppm) than Crater Lake and F much higher (maximum 2400 ppm). On the basis of melt inclusion analyses Webster and Duffield (1991) reported preeruptive volatile concentrations of ≤2.7 wt% $H_2O$, 2500 ppm Cl, and 2600 ppm F in the 28 Ma highly differentiated Taylor Creek Rhyolite of New Mexico. The relatively high Cl/F of the Crater Lake and Taupo melt inclusions in comparison with Obsidian Dome, Bandelier, and Taylor Creek samples is consistent with dominance of Cl over F in arc environments and the importance of F in continental settings (Christiansen et al., 1983).

### Pressure and depth

Minimum pressures implied by $H_2O$ and $CO_2$ concentrations can be estimated from solubility relations for rhyolitic liquids (Blank et al., 1989; Silver et al., 1990). If we assume saturation with a $H_2O$-$CO_2$ vapor at 880 °C, equilibrium pressures for 3.9–5.3 wt% $H_2O$ in the liquid are 1.0–1.8 kbar for $CO_2^{melt} = 0$ and 1.1–1.9 kbar for $CO_2^{melt} = 50$ ppm (Table 4). These pressures correspond to depths of 5–9 km for a bulk density of upper crustal volcanic rocks of 2.2 g·cm$^{-3}$ (Williams et al., 1987). Thus, the top of the climactic magma chamber was ≥5 km below the ground surface.

### $H_2O$ speciation in melt inclusions

The ratio of molecular $H_2O$ to OH groups dissolved in glass is temperature dependent (Zhang et al., 1991). Speciation data are plotted in Figure 3. The speciation results indicate the final cooling history of the inclusions whether or not inclusions leaked before cooling. The melt inclusions indicate closure temperatures for $H_2O$ speciation of 200–500 °C. The inclusions studied by Anderson et al. (1989) in quartz phenocrysts in Plinian pumice of the Bishop Tuff overlap this temperature range. The fall deposits from which pumice samples were collected at Crater Lake are nonwelded, although the climactic pumice

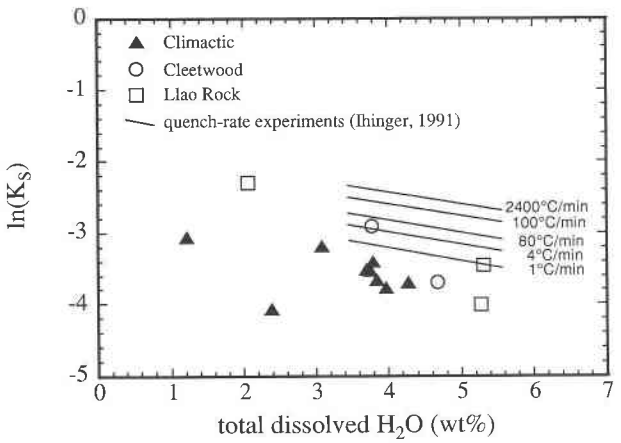


Fig. 4. Comparison of the speciation of $H_2O$ in Crater Lake melt inclusions with that of glassy products of quench-rate experiments by Ihinger (1991).

$$\ln K_s = \ln \frac{(X_{OH^{melt}})^2}{(X_{O^{melt}}) \times (X_{H_2O^{melt}})}$$

where $X_{i^{melt}}$ is the mole fraction of species $i$ in the melt. The shapes of the lines drawn for the constant quench rates are schematic.

fall, particularly near its base, tends to be slightly pinkish in color and forms steeper slopes than the Cleetwood or Llao Rock deposits as though it was hotter when deposited (recall that sample localities are near vent sites). The highest closure temperatures shown in Figure 3 are for an inclusion in early pumice from the Llao Rock deposit and for one of two inclusions in a single pumice lump from the Cleetwood deposit. The generally lower temperatures recorded by climactic pumice may result from slower postdepositional cooling. Indeed, a comparison of these results with quench-rate data from Ihinger (1991) suggests that cooling rates for the inclusions from the climactic eruption were slower than 1 °C/min, whereas those for some pumice clasts of the Cleetwood and Llao Rock eruptions were much faster (as fast as ~100 °C/min) (Fig. 4). Cooling of climactic inclusions through closure temperatures therefore must have occurred predominantly after deposition.

### Degassing during the climactic eruption

It was noted above that melt inclusions in all clasts examined from nonwelded exposures of the Wineglass Welded Tuff and the ignimbrite of the ring-vent phase of the climactic eruption are vesiculated. The majority can be seen to have leaked to the outsides of fractured crystals. This is particularly spectacular in late-erupted crystal-rich scoriae (Druitt and Bacon, 1989) in which melt inclusions are larger and more common than in phenocrysts in rhyodacitic pumices (although resorption of crystals results in some ambiguities in interpretation of textures in thin sections of scoriae). A plausible explanation for the vesiculation and fracturing is that of differential vapor pressure between melt trapped as inclusions and that outside of the crystals (Tait, 1992): depressurization of the magma allowed melt inclusions literally to blow apart their host crystals. Because this process affected all ignimbrite inclusions examined but only affected some of the inclusions in phenocrysts in Plinian pumices, it seems possible that vesiculation and leaking of melt inclusions in later erupted materials took place in the chamber because of degassing and depressurization of the magma during the Plinian phase of the climactic eruption.

The amount of Cl lost to the atmosphere during the climactic eruption may be estimated from the difference between Cl concentrations in melt inclusions and degassed Cleetwood vitrophyre. This value is ~1000 ppm. If all ~50 km³ of erupted magma degassed to this degree, ~$10^8$ tons of Cl entered the atmosphere.

## Acknowledgments

We thank John Armstrong and Paul Carpenter for aid with electron microprobe analyses. C.R.B. would like to express his gratitude for a Visiting Professorship with the Division of Geological and Planetary Sciences, Caltech. The manuscript was improved as a result of reviews by W.A. Duffield and J.B. Lowenstern and journal reviews by N.W. Dunbar and M.C. Johnson. Support for this work came from NSF grant EAR-8916707 from the Earth Sciences program and DOE grant DE-FG03-85ER13445. This is contribution no. 5168 of the Division of Geological and Planetary Sciences of the California Institute of Technology.

## References cited

Anderson, A.T., Jr. (1984) Probable relations between plagioclase zoning and magma dynamics, Fuego Volcano, Guatemala. American Mineralogist, 69, 660–676.

——— (1991) Hourglass inclusions: Theory and application to the Bishop Rhyolitic Tuff. American Mineralogist, 76, 530–547.

Anderson, A.T., Jr., Newman, S., Williams, S.N., Druitt, T.H., Skirius, C., and Stolper, E. (1989) $H_2O$, $CO_2$, Cl, and gas in Plinian and ash-flow Bishop rhyolite. Geology, 17, 221–225.

Armstrong, J.T. (1982) New ZAF and $\alpha$-factor correction procedures for the quantitative analysis of individual microparticles. In K.F.J. Heinrich, Ed., Microbeam analysis—1982, p. 175–180. San Francisco Press, San Francisco.

——— (1988) Quantitative analysis of silicate and oxide materials: Comparison of Monte Carlo, ZAF, and $\phi(\rho z)$ procedures. In D.E. Newbury, Ed., Microbeam analysis—1988, p. 239–246. San Francisco Press, San Francisco.

Bacon, C.R. (1983) Eruptive history of Mount Mazama and Crater Lake caldera, Cascade Range, U.S.A. Journal of Volcanology and Geothermal Research, 18, 57–115.

Bacon, C.R., and Druitt, T.H. (1988) Compositional evolution of the zoned calcalkaline magma chamber of Mount Mazama, Crater Lake, Oregon. Contributions to Mineralogy and Petrology, 98, 224–256.

Bacon, C.R., and Lanphere, M.A. (1990) The geologic setting of Crater Lake, Oregon. In E.T. Drake, R. Collier, J. Dymond, and G.L. Larson, Eds., Crater Lake: An ecosystems study, p. 19–27. American Association for the Advancement of Science, Pacific Division, San Francisco.

Blank, J.G., Stolper, E.M., Sheng, J., and Epstein, S. (1989) The solubility of $CO_2$ in rhyolitic melt at pressures to 1500 bars. Geological Society of America Abstracts with Programs, 21, A157.

Bruggman, P.E., Bacon, C.R., Aruscavage, P.J., Lerner, R.W., Schwarz, L.J., and Stewart, K.C. (1987) Chemical analyses of rocks and glass separates from Crater Lake National Park and vicinity, Oregon. U.S. Geological Survey Open-File Report 87-57, 36 p.

Christiansen, E.H., Burt, D.M., Sheridan, M.F., and Wilson, R.T. (1983) The petrogensis of topaz rhyolites in the western United States. Contributions to Mineralogy and Petrology, 83, 16–30.

Dobson, P.F., Epstein, S., and Stolper, E.M. (1989) Hydrogen isotope

fractionation between coexisting vapor and silicate glasses and melts at low pressure. Geochimica et Cosmochimica Acta, 53, 2723–2730.

Druitt, T.H., and Bacon, C.R. (1986) Lithic breccia and ignimbrite erupted during the collapse of Crater Lake caldera, Oregon. Journal of Volcanology and Geothermal Research, 29, 1–32.

——(1989) Petrology of the zoned calcalkaline magma chamber of Mount Mazama, Crater Lake, Oregon. Contributions to Mineralogy and Petrology, 101, 245–259.

Dunbar, N.W., Hervig, R.L., and Kyle, P.R. (1989) Determination of pre-eruptive $H_2O$, F and Cl contents of silicic magmas using melt inclusions: Examples from Taupo volcanic center, New Zealand. Bulletin of Volcanology, 51, 177–184.

Harris, D.M., and Anderson, A.T., Jr. (1983) Concentrations, sources, and losses of $H_2O$, $CO_2$, and S in Kilauean basalt. Geochimica et Cosmochimica Acta, 47, 1139–1150.

——(1984) Volatiles, $H_2O$, $CO_2$, and Cl in a subduction related basalt. Contributions to Mineralogy and Petrology, 87, 120–128.

Hervig, R.L., and Dunbar, N.W. (1989) Direct determinations of volatile gradients in the Bandelier Tuff through analysis of melt inclusions. International Association of Volcanology and Chemistry of the Earth's Interior General Assembly Abstracts, New Mexico Bureau of Mines and Mineral Resources Bulletin 131, 129.

Hervig, R.L., Dunbar, N.W., Westrich, H.R., and Kyle, P.R. (1989) Pre-eruptive water content of rhyolitic magmas as determined by ion microprobe analyses of melt inclusions in phenocrysts. Journal of Volcanology and Geothermal Research, 36, 293–302.

Ihinger, P.D. (1991) An experimental study of the interaction of water with granitic melt, 188 p. Ph.D. thesis, California Institute of Technology, Pasadena.

Love, G., Cox, M.G., and Scott, V.D. (1978) A versatile atomic number correction for electron-probe microanalysis. Journal of Physics D, 11, 7–27.

Lowenstern, J.B., and Mahood, G.A. (1991) New data on magmatic $H_2O$ contents of pantellerites, with implications for petrogenesis and eruptive dynamics at Pantcleria. Bulletin of Volcanology, 54, 78–83.

Merzbacher, C., and Eggler, D.H. (1984) A magmatic geohygrometer: Application to Mount St. Helens and other dacitic magmas. Geology, 12, 587–590.

Newman, S., and Chesner, C. (1989) Volatile compositions of glass inclusions from the 75Ka Toba Tuff, Sumatra. Geological Society of America Abstracts with Programs, 21, A271.

Newman, S., Epstein, S., and Stolper, E. (1986) Measurement of water in rhyolitic glasses: Calibration of an infrared spectroscopic technique. American Mineralogist, 71, 1527–1541.

——(1988) Water, carbon dioxide, and hydrogen isotopes in glasses from the ca. 1340 A.D. eruption of the Mono Craters, California: Constraints on degassing phenomena and initial volatile content. Journal of Volcanology and Geothermal Research, 35, 75–96.

Qin, Z., Lu, F., and Anderson, A.T., Jr. (1992) Diffusive reequilibration of melt and fluid inclusions. American Mineralogist, 77, 565–576.

Reed, S.J.B. (1965) Characteristic fluorescence correction in electron-probe microanalysis. British Journal of Applied Physics, 16, 913–926.

Rutherford, M.J., and Devine, J.D. (1988) The May 18, 1980, eruption of Mount St. Helens 3. Stability and chemistry of amphibole in the magma chamber. Journal of Geophysical Research, 93, 11949–11959.

Rutherford, M.J., Sigurdsson, H., Carey, S., and Davis, A. (1985) The May 18, 1980, eruption of Mount St. Helens 1. Melt composition and experimental phase equilibria. Journal of Geophysical Research, 90, 2929–2947.

St. Seymour, K., and Vlassopoulos, D. (1989) The potential for future explosive volcanism associated with dome growth at Nisyros, Aegean volcanic arc, Greece. Journal of Volcanology and Geothermal Research, 37, 351–364.

Silver, L.A., Ihinger, P.D., and Stolper, E. (1990) The influence of bulk composition on the speciation of water in silicate glasses. Contributions to Mineralogy and Petrology, 104, 142–162.

Skirius, C.M. (1990) Pre-eruptive $H_2O$ and $CO_2$ content of Plinian and ash-flow Bishop Tuff magma, 237 p. Ph.D. thesis, University of Chicago, Chicago.

Sommer, M.A. (1977) Volatiles $H_2O$, $CO_2$, and CO in silicic melt inclusions in quartz phenocrysts from the rhyolitic Bandelier air-fall and ash-flow tuff, New Mexico. Journal of Geology, 85, 423–432.

Sommer, M.A., and Schramm, L.S. (1983) An analysis of the water concentrations in silicate melt inclusions in quartz phenocrysts from the Bandelier Tuff, Jemez Mts., New Mexico. Bulletin of Volcanology, 46, 299–320.

Tait, S. (1992) Selective preservation of melt inclusions in igneous phenocrysts. American Mineralogist, 77, 146–155.

Vogel, T.A., Mills, J.G., Jr., Aines, R.D., and Merzbacher, C.I. (1989) Pre-eruptive volatiles in a chemically zoned magma body based on melt inclusions. Geological Society of America Abstracts with Programs, 21, A271.

Webster, J.D., and Duffield, W.A. (1991) Volatiles and lithophile elements in Taylor Creek Rhyolite: Constraints from glass inclusion analysis. American Mineralogist, 76, 1628–1645.

Webster, J.D., and Holloway, J.R. (1990) Partitioning of F and Cl between magmatic-hydrothermal fluids and highly evolved granitic magmas. Geological Society of America Special Paper 246, 21–34.

Williams, D.L., Abrams, G., Finn, C., Dzurisin, D., Johnson, D.J., and Denlinger, R. (1987) Evidence from gravity data for an intrusive complex beneath Mount St. Helens. Journal of Geophysical Research, 92, 10207–10222.

Williams, H. (1942) The geology of Crater Lake National Park, Oregon. Carnegie Institution of Washington Publication 540, 162 p.

Young, S.R. (1990) Physical volcanology of Holocene airfall deposits from Mt. Mazama, Crater Lake, Oregon, 298 p. Ph.D. thesis, University of Lancaster, Lancaster, U.K.

Zhang, Y., Stolper, E.M., and Wasserburg, G.J. (1991) Diffusion of water in rhyolitic glasses. Geochimica et Cosmochimica Acta, 55, 441–456.

Manuscript received December 2, 1991
Manuscript accepted May 12, 1992